Impact of heterogeneity, bed forms, and stream curvature on subchannel hyporheic exchange

M. Bayani Cardenas[1] and J. L. Wilson

Department of Earth and Environmental Science, New Mexico Institute of Mining and Technology, Socorro, New Mexico, USA

V. A. Zlotnik

Department of Geosciences, University of Nebraska at Lincoln, Lincoln, Nebraska, USA

Received 5 January 2004; revised 24 May 2004; accepted 9 June 2004; published 18 August 2004.

[1] Advection through hyporheic zones (HZ) consisting of heterogeneous channel bend streambed deposits and their equivalent homogenous medium was investigated using finite difference groundwater flow and transport simulations and forward particle tracking. The top prescribed head boundary was varied in order to mimic various stream channel head distributions resulting from the presence of bed forms and channel curvature. Flux calculations show that heterogeneity causes significant additional HZ flux compared to an equivalent homogenous medium. However, the major cause of HZ flux is a spatially periodic (sinusoidal) head distribution along the boundary, representing the effect of bed forms. The additional influence of heterogeneity on the total channel-bed exchange and the overall HZ geometry are increased when boundary head sinusoidal fluctuation is more subdued. We present dimensionless numbers that summarize these relationships. Heterogeneity's influence is further magnified by considering the effect of channel curvature on boundary heads. The simulations illustrate the dynamic influence of heterogeneity on the hyporheic zone since the various head boundaries employed in our modeling efforts are a proxy for different surface water conditions and bed form states that may occur during a single flood. Furthermore, we show that residence times (total tracking times) of particles originating from the streambed follow a lognormal distribution. In the presence of heterogeneity, residence times can decrease or they can increase compared to residence times for homogeneous conditions depending on the relative positions of the heterogeneities and the bed forms. Hence streambed heterogeneity and stream curvature, factors often neglected in previous modeling efforts, combine with bed form configuration to dynamically determine HZ geometry, fluxes, and residence time distributions. *INDEX TERMS:* 1829 Hydrology: Groundwater hydrology; 1832 Hydrology: Groundwater transport; 1860 Hydrology: Runoff and streamflow; 5114 Physical Properties of Rocks: Permeability and porosity; *KEYWORDS:* hyporheic zone, heterogeneity, bed forms, stream curvature, fluxes, residence times

Citation: Cardenas, M. B., J. L. Wilson, and V. A. Zlotnik (2004), Impact of heterogeneity, bed forms, and stream curvature on subchannel hyporheic exchange, *Water Resour. Res.*, *40*, W08307, doi:10.1029/2004WR003008.

1. Introduction

1.1. Relevance and Previous Work

[2] A "hyporheic zone" (or HZ for brevity) is an area where water infiltrates from streams then flows through streambed sediments and stream banks and returns to the surface after relatively short pathways. These zones are important for two major reasons. They provide hyporheic and riparian organisms critical solutes, including nutrients, and dissolved gases [*Triska et al.*, 1989, 1993; *Findlay*, 1995; *Harvey and Fuller*, 1998; *Doyle et al.*, 2003]; they also control the distribution of solutes and colloids from bed form to watershed scales [*Elliot and Brooks*, 1997a; *Woessner*, 2000; *Packman and Brooks*, 2001; *Sophocleous*, 2002; *Kasahara and Wondzell*, 2003]. Understanding of HZ exchange improves through integrated modeling and field observations, supported by laboratory experiments.

[3] Several methods have been proposed for modeling hyporheic exchange and are reviewed by *Packman and Bencala* [2000]. Among the simplest of models are those that describe the exchange of solutes between rivers and adjacent transient storage zones as linear first-order mass transfer processes with lumped exchange coefficients, such as those by *Bencala and Walters* [1983] or *Young and Wallis* [1993]. Exchange models based on one-dimensional diffusive processes, transverse to the channel, are slightly more sophisticated [*Worman*, 1998; *Jonsson et al.*, 2003]. Other models consider the effects of early non-Fickian transport of

[1]Also at New Mexico Bureau of Geology and Mineral Resources, New Mexico Institute of Mining and Technology, Socorro, New Mexico, USA.

0043-1397/04/2004WR003008$09.00

solutes from the substratum to the stream [*Richardson and Parr*, 1988]. Parameters in these models are determined by empirically matching model output to actual solute breakthrough curves in laboratory experiments [*Marion et al.*, 2002] and detailed field experiments [*Harvey et al.*, 1996; *Choi et al.*, 2000; *Jonsson et al.*, 2003]. In certain settings, empirical determination of these parameters is not straightforward, and sometimes not possible, suggesting that these models are conceptually inconsistent with some environments [*Harvey and Fuller*, 1998; *Harvey and Wagner*, 2000]. A major source of discrepancy is that these simple models do not completely and realistically represent the hydrodynamics involved in hyporheic exchange.

[4] In some cases, exchange processes between streams and aquifers are dominated by advection rather than diffusion. Two important mechanisms for this type of hyporheic exchange have been proposed. The first is driven by advective flow induced by head gradients which are in turn generated by streambed topography due to bed forms or other irregularities such as logs and boulders and/or water surface topography. The second is due to the dynamic behavior of bed forms which temporarily trap and release water as they migrate. These two mechanisms are referred to as ''pumping'' and ''turnover'' [*Elliot and Brooks*, 1997a; *Packman and Brooks*, 2001].

[5] Several studies have investigated the mechanics of pumping from a theoretical perspective, often supported by experiments. *Ho and Gelhar* [1973] present results of analytical and experimental studies on turbulent flow with wavy permeable boundaries. *Thibodeaux and Boyle* [1987] propose a simple physically based model supported by laboratory observations. *Shum* [1992] examines the effects of the passage of progressive gravity waves on advective transport in a porous bed. *Savant et al.* [1987], applying the boundary element numerical method, replicate flume observations of flow along a vertical plane induced by head fluctuations. More sophisticated analytical models, supported by flume experiments and numerical modeling, consider the transfer of solutes and colloids through mobile bed forms [*Elliot and Brooks*, 1997a, 1997b; *Packman and Brooks*, 2001]. *Worman et al.* [2002] presents a model that couples longitudinal solute transport in streams with solute advection along a continuous distribution of hyporheic flow paths. All of these theoretical, experimental and numerical studies are confined to two-dimensional (2-D) vertical domains, taken longitudinally along the channel, either due to their experimental setup or to enable simpler theoretical or numerical analyses.

[6] There has also been considerable work on 2-D essentially horizontal flow models. Examples of reach-scale 2-D numerical modeling of hyporheic exchange are given by *Harvey and Bencala* [1993], *Wondzell and Swanson* [1996], and *Wroblicky et al.* [1998]. The first example conceptually studies the impact of stepped-channels on surface-subsurface exchange. The last two examples are based on extensive data sets that allowed calibration of the flow models. All three cases demonstrate the viability of using numerical models to simulate horizontal flow into, through and out of channel banks while neglecting vertical exchange.

[7] There are a few fully three-dimensional (3-D) simulations of hyporheic exchange. For example, there are channel-scale (hundreds of meters) studies by *Storey et al.* [2003], who investigate key factors controlling hyporheic exchange, and by *Kasahara and Wondzell* [2003], who examine the impacts of morphologic features. *Storey et al.* [2003] demonstrate that the homogeneous hydraulic conductivity (K) of the alluvial deposits controls the rate and extent of hyporheic exchange; no hyporheic exchange will occur if the K of the streambed is below a certain threshold.

[8] Some of the models mentioned above consider heterogeneity at larger spatial scales. For instance, *Kasahara and Wondzell* [2003] interpolated slug test data by assigning K values to regions around wells using the Thiessen Polygon method. *Storey et al.* [2003] employed spatially variable aquifer and streambed hydraulic properties that varied at a scale on the order of tens of meters. However, owing to their scales and resolution, all of these models ignore the finer-scale heterogeneity typical of streambeds [*Bridge*, 2003]. This limitation is widely recognized by investigators of hyporheic processes, and is best summarized by *Packman and Bencala* [2000, p. 51]: ''Some additional complexities typically found in the natural environment, such as heterogeneity in the bed sediment, have also been omitted from the current models. Thus, even though these models are useful because they include process-level understanding, their application has been limited.'' Even earlier *Harvey and Bencala* [1993, p. 96] stated ''. . .the influence of heterogeneous hydraulic properties of the alluvium on surface-subsurface water exchange is a high priority to be considered in future research.'' Is there field evidence to confirm this speculation on the importance of heterogeneity? *White*'s [1993] observed temperature distributions at a site in the Maple River, northern Michigan, from which he inferred HZ geometry, appear to confirm this importance. Stronger confirmation comes from field tracer tests by *Wagner and Bretschko* [2002] which suggest that bed-scale variability of K results in a complex 3-D network of flow paths, and from which they deduce that heterogeneity is responsible for the patchy distribution of benthic invertebrates at their study site in Austria. What modeling has been done to test the importance of heterogeneity? A recent compilation of research on modeling of HZ processes listed no efforts addressing issues relating to streambed heterogeneity [*Runkel et al.*, 2003]. However, there are a few ongoing investigations that tackle these issues [*Matos et al.*, 2003; *Salehin et al.*, 2003].

[9] Conceptual understanding of hyporheic processes can only be further broadened if multidimensional analyses including heterogeneity are pursued [*Sophocleous*, 2002]. Numerical modeling of hyporheic flow is a viable solution to this impasse since it allows flexibility in the parameters and processes that can be investigated [*Packman and Bencala*, 2000]. Previous modeling efforts by *Woessner* [2000] elucidated this. He introduced high K rectangles set in a matrix of lower K. A linear head gradient was then imposed on the top boundary of the two-dimensional vertical section. A no-flow boundary was set at the downstream end of the domain in order to generate return flow to the river. This resulted in flow lines that are similar to field observations [see *Woessner*, 2000, Figures 5 and 6] although the model conditions, i.e., no flow at the down-

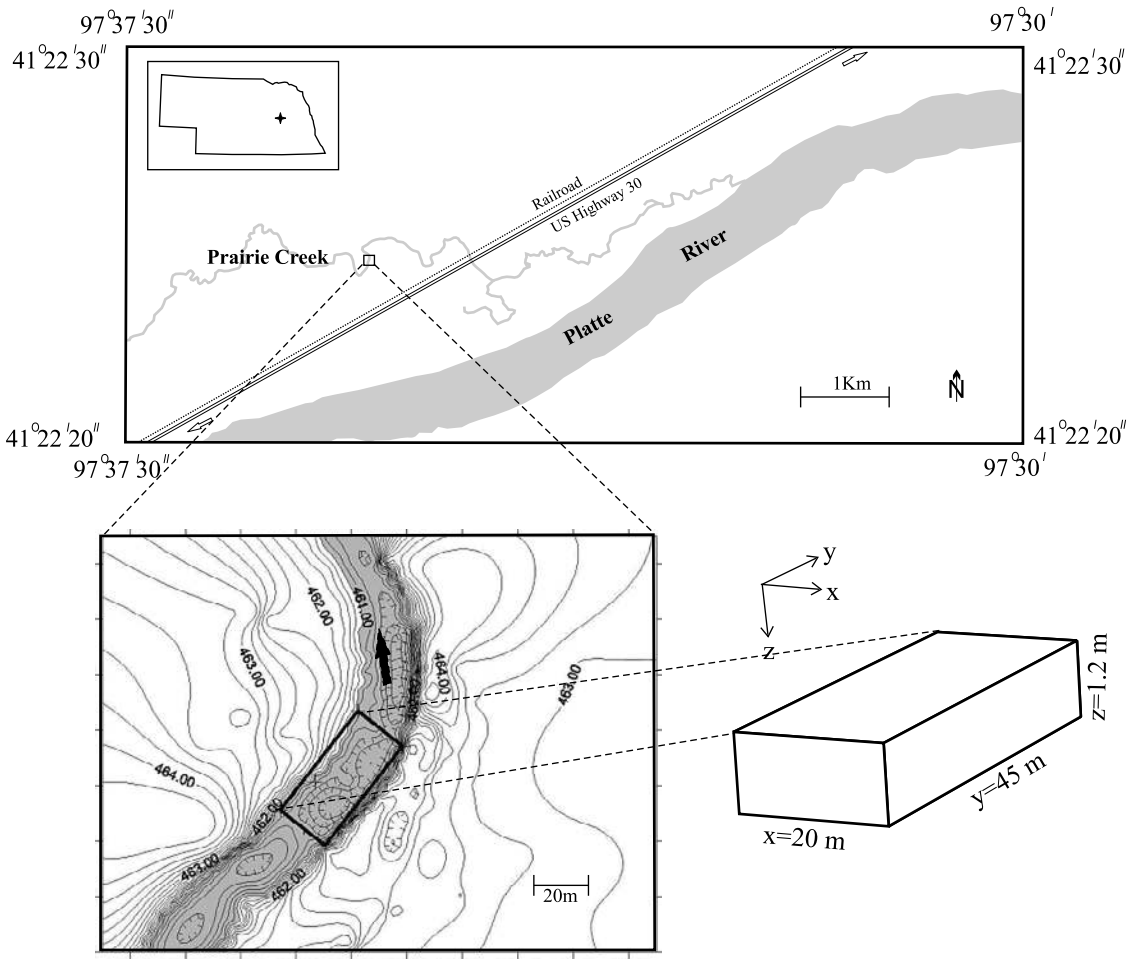

Figure 1. Topographic map of the Prairie Creek test site, Nebraska (elevation in m; contour interval = 0.2 m). Enlarged rectangular block is the model domain.

stream end and a binary K field, are only a crude approximation of natural conditions.

1.2. Purpose of This Study

[10] Previous studies have not exploited the capability of groundwater flow models to explicitly consider bed-scale 3-D spatial variability in hydraulic properties of the subchannel HZ. Partly, this owes to the extensive fieldwork necessary for the data intensive sedimentological models necessary to represent realistic spatial heterogeneity of streambed hydraulic conductivity. Thus several fundamental questions remain unanswered. Under what conditions does heterogeneity induce substantial hyporheic exchange? Is the influence of heterogeneity on hyporheic flow comparable to the control exerted by bed or water surface topography, including the effects of bed forms and channel curvature? How are HZ geometry, streambed flux, and the HZ residence time of surface water controlled by each of these influences? In particular, when can we neglect and when should we consider heterogeneity, and channel curvature, in models of hyporheic processes? How do these answers change during the dynamic events of a flood with its evolving boundary condition at the streambed? The purpose of this paper is to provide some tentative answers to these questions based on modeling efforts using previously published field observations of heterogeneous streambed conductivity.

2. Methodology

2.1. Background and Model Hydraulic Properties

[11] We used a heterogeneous 3-D reconstruction of modern channel bend deposits developed by *Cardenas and Zlotnik* [2003a] for the flow and transport simulations. Their reconstruction is based on numerous constant head injection tests [*Cardenas and Zlotnik*, 2003b] and ground-penetrating radar surveys of Prairie Creek in central Nebraska (Figure 1). The interpolated hydraulic conductivity data compared favorably with data collected from surficial deposits in similar environments. The Prairie Creek's streambed is dominantly sand with some gravel and is typical of the small low-gradient streams traversing the mid-Western United States in contrast with the steep gravel bedded headwater streams where most field experiments on hyporheic exchange had been conducted. Its discharge varies from dry conditions during the summer irrigation season to 50 m^3/s when large storms pass through its 250 km^2 drainage area.

[12] We subdivided the reconstruction into 11 K values (Figure 2), which range from 2.5 m/d to 52.5 m/d, in our

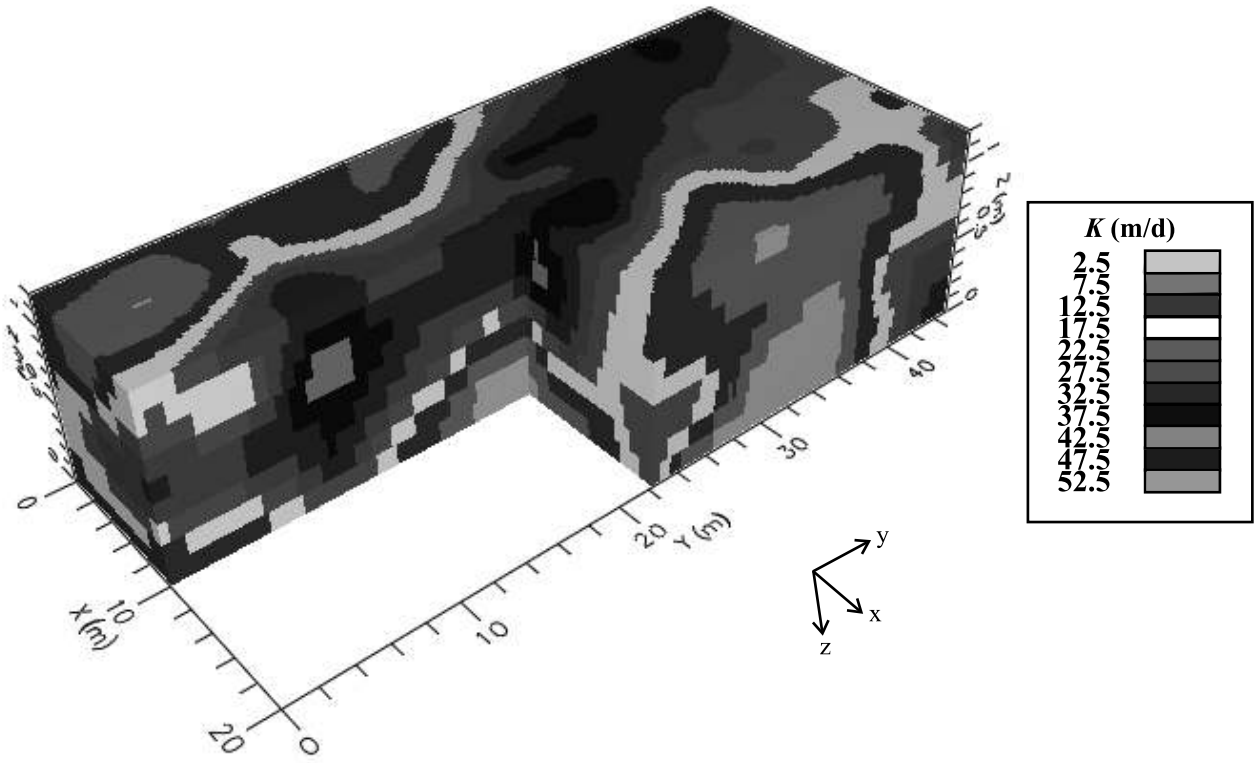

Figure 2. Model domain with three-dimensional hydraulic conductivity field. See color version of this figure at back of this issue.

domain. An equivalent homogeneous medium, with a K of 18 m/d assigned throughout the domain, was used as a control. Equivalence of the heterogeneous medium was accomplished through both volumetric averaging and numerical Darcian approaches [*Cardenas and Zlotnik*, 2003a]. All K values were locally isotropic as justified by the measurement scale of the instruments for hydraulic testing and the results of upscaling calculations. Effective porosity was 0.3 throughout the domain.

2.2. Flow and Transport Modeling

[13] We used the finite difference code MODFLOW [*McDonald and Harbaugh*, 1996] for flow modeling, MT3D99 [*Zheng*, 1999] for transport simulation, ZONEBUDGET [*Harbaugh*, 1990] for calculation of fluxes, and MODPATH [*Pollock*, 1994] for forward particle tracking. Solute transport in MT3D99 was simulated with a third-order total-variation-diminishing (TVD) scheme. Data processing and code execution were handled through the Visual MODFLOW user interface [*Waterloo Hydrogeologic, Inc.*, 2000].

[14] The model domain is 45 m × 20 m × 1.2 m (Figure 2). Each block is 25 cm × 25 cm × 4 cm (Δx, Δy, and Δz). These blocks are smaller (finer resolution) than the horizontal and vertical block sizes of 0.5 m and 0.13 m, respectively, used by *Cardenas and Zlotnik* [2003a] for their upscaling work. We refined the horizontal grid resolution so that sinusoidal prescribed head boundaries at the streambed interface would not become filtered. Vertical grid resolution was refined to limit solute numerical dispersion. We imposed a no-flow boundary at the bottom and prescribed heads at the remaining external faces of the domain. Varying the top boundary between simulations allowed us to represent various streambed interface conditions. Although somewhat arbitrary, the four external vertical faces were assigned the same heads as in the corresponding grid block in the top boundary.

[15] Simulations were designed to allow us to identify the effects of varying individual features including spatial heterogeneity, bed form configuration, and channel curvature. The initial simulations considered a top head boundary characterized by an along-stream or mean longitudinal gradient $J_y = -\partial h/\partial y$. We arbitrarily imposed a gradient of 0.011 (head is 3 m at y = 0 m and 2.5 m at y = 45 m). Although this gradient is high, it is about half of the gradient that *Woessner* [2000] used in his simulations, and in any event the results of this linear system simulation can be normalized by the gradient. We then superposed an across-stream or transverse gradient $J_x = -\partial h/\partial x$ to the previous top boundary in the second simulation. In streams, such a boundary will be generated due to the elevation of the water surface along the outer bank of a meander [*Bridge*, 1992]. In most simulations, we arbitrarily imposed a J_x of -0.01 (a change of 20 cm along the 20 m width), similar to the longitudinal gradient. We also ran low-gradient simulations. In these cases, the longitudinal and transverse gradients, respectively, were 0.0011 and -0.001 (a head change of 5 cm along the 45-m length and a head change of 2 cm

Table 1. Top Boundary Prescribed Head Conditions and Corresponding Steady State Fluxes

Model[a]	Figure[b]	K Field	J_x	J_y	A, m	λ, m	Flux,[c] m^3/d	N_E	z_{HZ}, m	N_H	N
A	4a and 5e	heterogeneous	-	−0.011	-	-	12.40	0.00	0	∞	∞
B	4b	heterogeneous	0.01	−0.011	-	-	18.06	0.00	0	∞	∞
C	4c and 5d	heterogeneous	-	−0.011	0.01	12.5	33.99	0.29	0.68	0.54	1.87
D	4d	homogeneous	-	−0.011	0.01	12.5	27.41	0.29	0.68	0.00	0.00
E		heterogeneous	-	−0.011	0.01	12.5[d]	29.34	0.29	0.68	0.54	1.87
F		homogeneous	-	−0.011	0.01	12.5[d]	24.74	0.29	0.68	0.00	0.00
G	4e	heterogeneous	0.01	−0.011	0.01	12.5	32.67	0.29	0.68	0.54	1.87
H	4f	homogeneous	0.01	−0.011	0.01	12.5	24.74	0.29	0.68	0.00	0.00
I	5a	heterogeneous	-	−0.011	0.02	2	709.45	3.64	1.04	0.36	0.10
J		homogeneous	-	−0.011	0.02	2	563.75	3.64	1.04	0.00	0.00
K	5b	heterogeneous	-	−0.011	0.01	2	356.06	1.82	0.88	0.42	0.23
L		homogeneous	-	−0.011	0.01	2	282.86	1.82	0.88	0.00	0.00
M		heterogeneous	0.01	−0.011	0.01	2	356.23	1.82	0.84	0.44	0.24
N		homogeneous	0.01	−0.011	0.01	2	282.98	1.82	0.84	0.00	0.00
O	5c	heterogeneous	-	−0.011	0.01	6.2	91.72	0.59	0.88	0.42	0.72
P		homogeneous	-	−0.011	0.01	6.2	78.13	0.59	0.88	0.00	0.00
Q		heterogeneous	0.01	−0.011	0.01	6.2	92.78	0.59	0.88	0.42	0.72
R		homogeneous	0.01	−0.011	0.01	6.2	78.44	0.59	0.88	0.00	0.00
S		heterogeneous	-	−0.0011	-	-	1.27	0.00	0	∞	∞
T		heterogeneous	0.001	−0.0011	-	-	1.94	0.00	0	∞	∞
U		homogeneous	0.001	−0.0011	0.005	6.2	39.04	2.93	1.2	0.00	0.00
V		heterogeneous	0.001	−0.0011	0.005	6.2	45.55	2.93	1.2	0.31	0.11

[a]Same designation in Figures 6 and 7.
[b]Designations in Figures 4 and 5.
[c]Flux = inflow $\cong$ outflow.
[d]Shifted by half a wavelength.

along the 20-m width), an order of magnitude smaller than most of our simulations but identical once normalized.

[16] On the basis of the models for advective flow through stream bottoms, as well as actual observations, head fluctuations due to irregularities of the bed or water surface pump water into and out of HZs. These head fluctuations are commonly idealized in theoretical models and represented as a harmonic function imposed on a flat surface [*Ho and Gelhar*, 1973; *Shum*, 1992; *Elliot and Brooks*, 1997a; *Packman and Brooks*, 2001]. A larger-scale analogue of this technique of approximating topographic variations by imposing sinusoidal head fluctuations on a flat boundary can be traced back to *Tóth* [1963]. We similarly represented this effect by superimposing a sinusoidal head boundary to the linear gradient as described by the following equation:

$$h = b - J_y y + A \sin(\omega y) \quad (1)$$

where h is the head at longitudinal location y, b is the head at the upstream boundary, and A is the amplitude of the fluctuations. The angular frequency is defined by $\omega = 2\pi/\lambda$ where λ is the wavelength. Conditions for the various simulations are given in Table 1. While we have used a reconstructed streambed from the Prairie Creek, there were no quantitative field observations of stream flow, bed topography, and porous media head distributions. The simulation boundary conditions and results are hypothetical and do not reproduce field conditions.

[17] We followed *Woessner*'s [2000] approach to illustrate the 3-D morphology of the HZ with a constant-concentration (Dirichlet) boundary of 100 mg/L at top of the domain to represent stream water and a background concentration of 0 mg/L (pure groundwater) throughout the rest of the domain at the start of each run. Dispersivity was set to zero since we want to study advective hyporheic exchange. Inflow and outflow boundaries, i.e., the side vertical boundaries, were considered as Cauchy type boundaries where the dispersive flux is ignored as this is customary in MT3D [*Zheng*, 1999]. The bottom was a no-flux boundary. Numerical dispersion was analyzed by comparing isoconcentration lines with path lines (see discussion below). All flow and transport simulations were executed to steady state. Flux calculations through the streambed were determined by assigning the top boundary as a "zone" in ZONEBUDGET.

[18] Residence time of water originating from the surface was determined through forward tracking of 1215 particles initially distributed uniformly on the top horizontal layer. The reported residence time was the total tracking time or the time it takes for the particle to exit the domain, which does not necessarily occur through the top boundary. Some particles continue traveling in the subsurface. Thus the tracking times are minimum residence times and some of the resulting distributions are biased.

3. Results and Discussion

3.1. Hyporheic Zone Morphology

[19] Longitudinal cross sections along x = 10 m in Figure 3 show that the 50 mg/L isoline mimics path lines originating from the top boundary, i.e., the stream, and coincides with the deepest path lines. We conclude that the 50 mg/L isoline/isosurface is an accurate representation of the area influenced by advection from the stream, i.e., the advective HZ. Minor discrepancies between the deepest path line and the 50 mg/L isoline in Figure 3b (heterogeneous case) arise from the projection of the path lines to the cross-sectional surface. Figures 4 and 5show the results of our steady state simulations (the letter designations in the Figures 4 and 5 correspond to those in the second column of Table 1). The shaded surfaces are the 50 mg/L isosurfaces and represent the extent of the advective subchannel HZs.

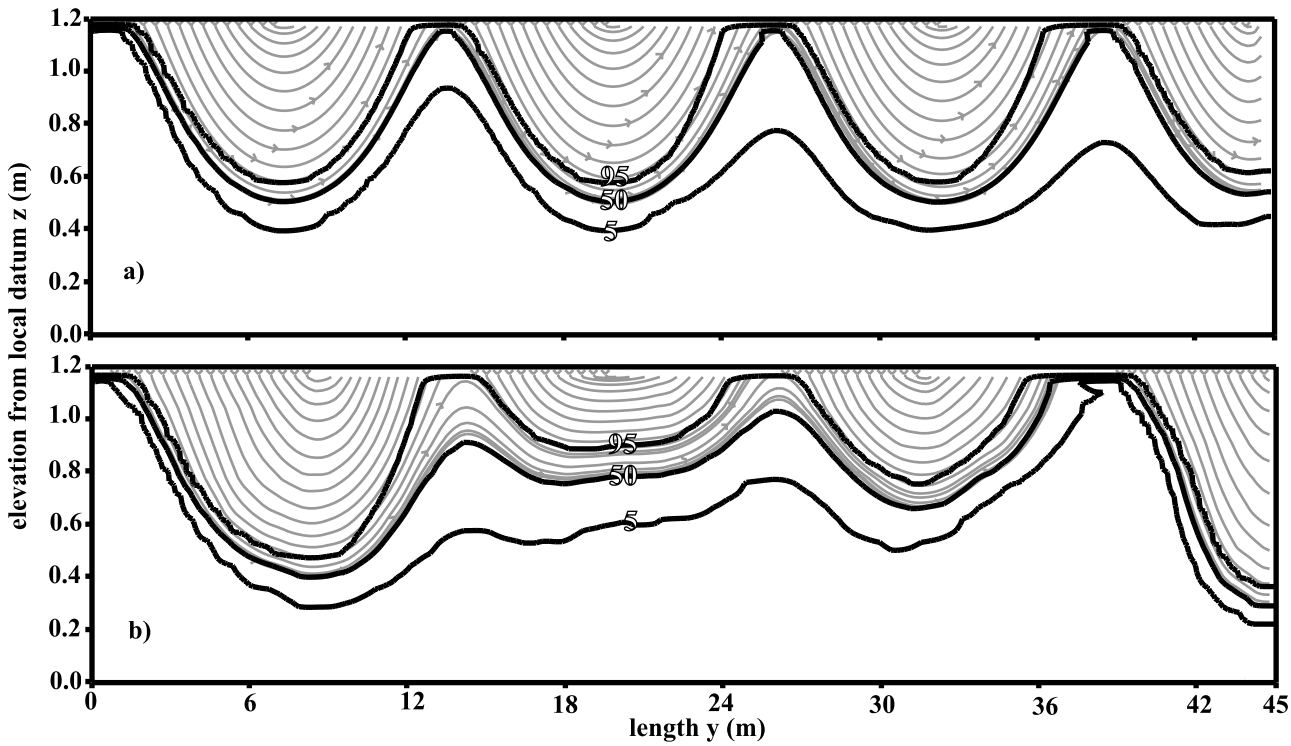

Figure 3. Longitudinal cross sections taken at x = 10 m: (a and b) Path lines (shaded) and isoconcentration lines (solid) for a homogeneous and heterogeneous domain, respectively. Top prescribed head boundary in Figures 3a and 3b is described by the same sinusoidal function.

[20] Imposing only a linear longitudinal head gradient on the top boundary of a homogeneous K field does not produce an advective HZ since the ''stream water'' in the first layer (top boundary) flows only horizontally. In this case subchannel HZs would only be produced by considering transverse diffusion and dispersion, processes which we ignore. However, inclusion of heterogeneity under the same boundary conditions does produce an advective HZ (Figure 4a). The geometry of this zone is reminiscent of *White*'s [1993] 3-D representation of the HZ based on temperature distribution. Clearly, heterogeneity determines the location of upwelling and downwelling areas. Figure 4b is based on similar conditions as in Figure 4a except that we add the effects of a raised surface water level (J_x) on one side of the channel due to channel curvature. Expectedly, the HZ deflects toward the point bar (see Figure 1 for orientation of domain along the channel) where the resulting gradient is directed. *Harvey and Bencala* [1993] and *Wroblicky et al.* [1998] observe and model flow through point bars. They show that hyporheic exchange is driven by the confluent effects of river geomorphology and the ambient down-valley gradient of groundwater (see *Larkin and Sharp* [1992] for more examples). Our results illustrate that the water surface topography along meanders also contributes to this exchange. Furthermore, the spatial pattern of K works in tandem with this effect since high-K areas, the locations of which are controlled by surface water dynamics, are aligned with the prevailing gradients caused by the stream's curvature.

[21] The effects of heterogeneity on HZ geometry are less prevalent when there is a sinusoidal head boundary representing the effects of bed forms and water surface topography (Figure 5). Increasing the frequency or amplitude of the sinusoidal fluctuations further reduces the influence of a heterogeneous K field. These relationships can be analyzed by introducing two dimensionless numbers that represent external forcing terms and internal spatial variability separately. The first number

$$N_E = \frac{2A/(\lambda/2)}{|J_y|} = \frac{4A}{\lambda|J_y|} \tag{2}$$

relates the local-scale forcing mechanism (gradient within half a wavelength of the sinusoidal head fluctuations) to the larger-scale forcing term (mean longitudinal gradient). The second number N_H assesses effects of heterogeneity on the geometry of the HZ by comparing the effects of vertical advection in the HZ due to bed forms with statistics summarizing the spatial variability of K:

$$N_H = \frac{\sigma^2_{\ln K} l_z}{z_{HZ}} \tag{3}$$

using two spatial scales, namely the HZ vertical extent z_{HZ} due to bed forms and the product of the variance, $\sigma^2_{\ln K}$, and vertical correlation length, l_z, of $\ln(K)$. For each particle tracking simulation, z_{HZ} was estimated as the location of the deepest point of all streamlines emanating from the streambed. z_{HZ} was determined for each homogeneous case and applied to its heterogeneous counterpart, to avoid double counting the influence of heterogeneity which is already represented in the numerator of equation (3). Finally, equations (2) and (3) can be combined as:

$$N = \frac{N_H}{N_E} = \frac{|J_y|\sigma^2_{\ln K} l_z \lambda}{4A z_{HZ}} \tag{4}$$

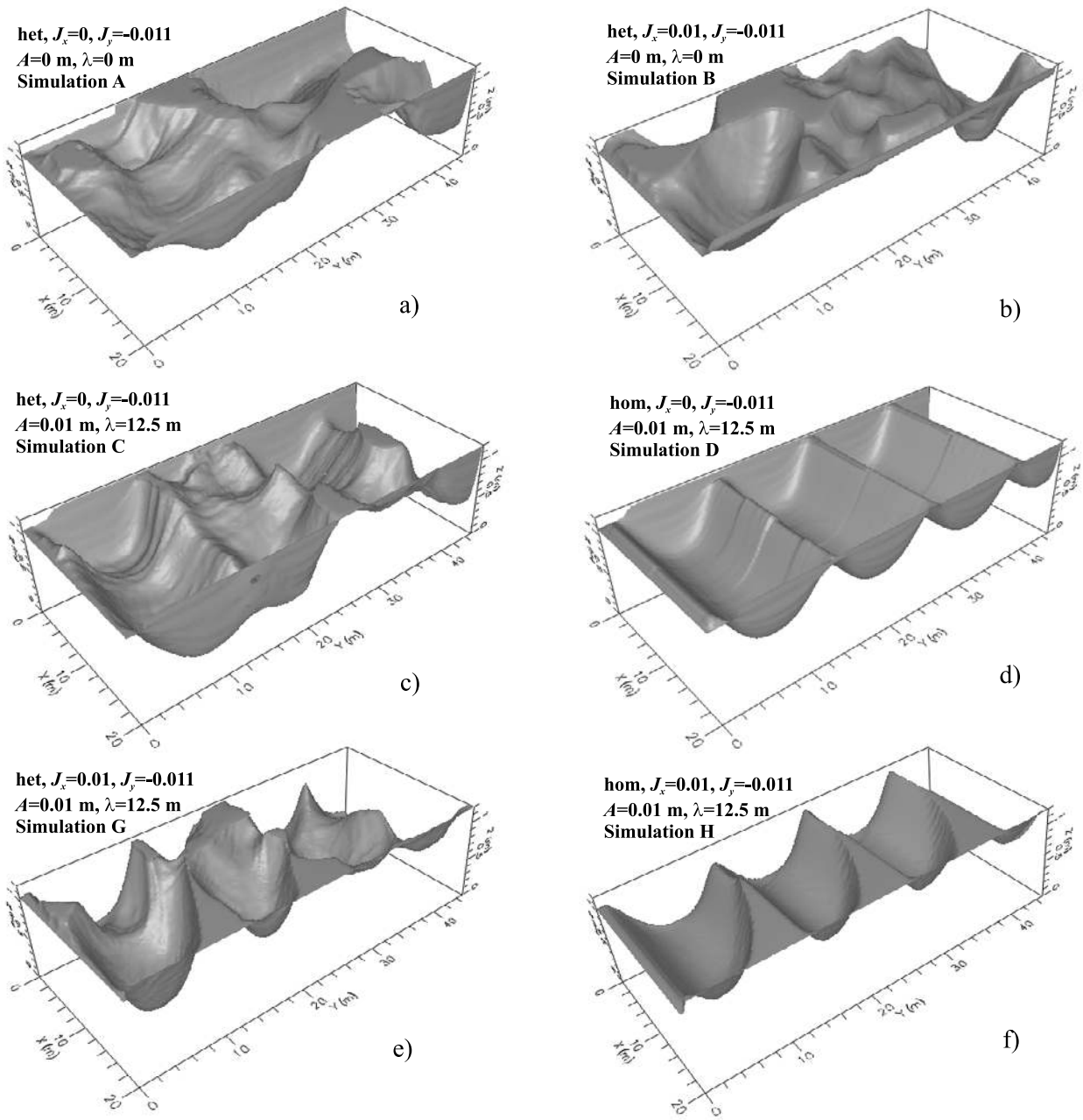

Figure 4. Steady state simulations results (see Table 1 for model conditions). The shaded surfaces are the 50 mg/L isosurfaces and represent the extent of the advective subchannel hyporheic zones. Model conditions and letter designations in Table 1 are shown beside the images.

Larger values of this dimensionless number indicate a significant heterogeneity induced HZ, which occurs when the variability of ln(K) is large and spatially correlated, and the frequency and amplitude of the sinusoidal head fluctuations are small. Missing from (4) is any consideration of the horizontal correlation lengths of ln(K).

[22] On the basis of the work of *Cardenas and Zlotnik* [2003a], $\sigma_{\ln K}$ = 0.86 and l_z = 0.5 m for the Prairie Creek streambed. N_H = 0 for the homogeneous cases. Likewise, N_E = 0 for cases where we don't consider a sinusoidal head distribution (no local gradients). Computations for N are presented in Table 1 and simulation examples are in Figure 5. The dimensionless numbers partly verify and summarize our observations. When N = 0, heterogeneity is clearly not a factor. As N increases, the influence of heterogeneity increases. When N is ∞, such as in cases A and B of Table 1 and Figure 5e, the advective HZ is driven completely by heterogeneity. Additional theoretical analysis or simulations considering various values for $\sigma_{\ln K}$ and l_z, and accounting for heterogeneity correlation in other directions (l_y and l_x), are needed to confirm the definition, significance and critical values of N.

[23] The usefulness of dimensionless N comes into play when the external driving mechanisms and internal

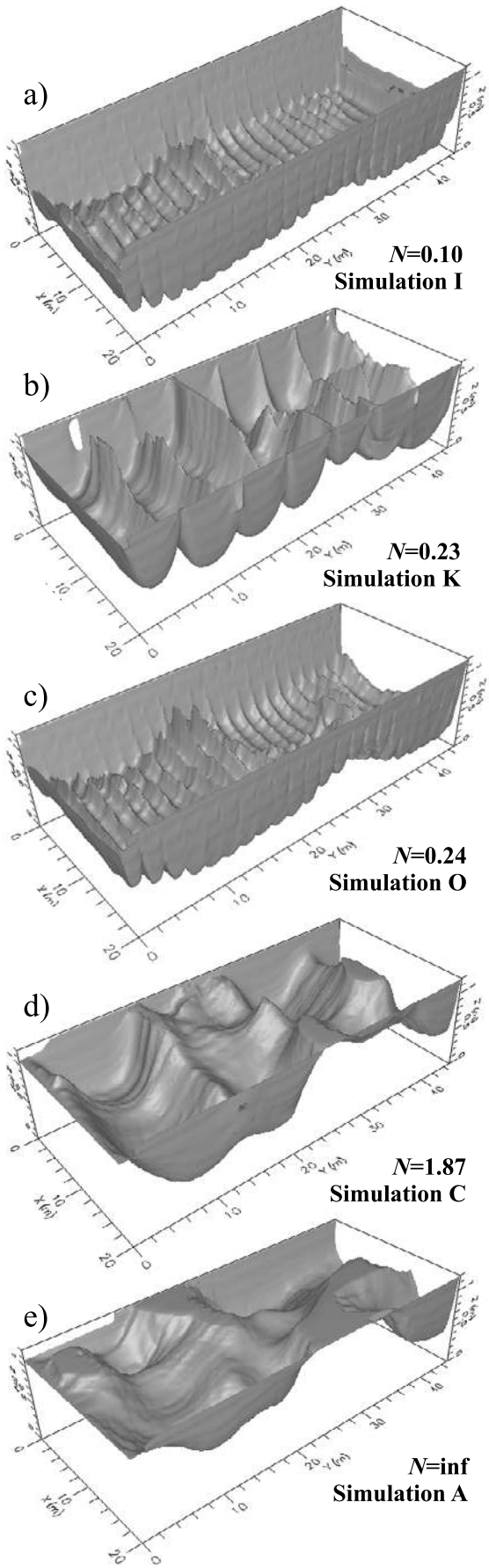

variability can be readily constrained, estimated, or are actually known a priori. For example estimation of N can help in the appropriate design of field experiments such as tracer tests. If estimated N is small the experimental design should put more weight on the configuration of the bed forms or other factors that cause head fluctuations. If estimated N is large any field campaign should take heterogeneity into consideration. N estimates could also be applied in the cross comparison of streams or stream reaches, and perhaps in biological diversity studies.

[24] Simulations A to R (Table 1 and Figures 4 and 5) illustrate the effects of some of the controlling factors on hyporheic flow in high-gradient streams. In the last series of simulations (S-V in Table 1) we attempted to simulate conditions that are more typical of lower gradient streams. Hyporheic zone geometry for simulations S and T are similar to Figures 4a and 4b since they are linearly scaled, thus confirming that heterogeneity is important in this setting. This further evinces that the HZ distribution is more sensitive to a heterogeneous K field if a linear gradient dominates over the local sinusoidal head field at the top boundary.

3.2. Implications on Short-Term Hyporheic Zone Dynamics

[25] *Wondzell and Swanson* [1999] observed changes in HZs due to dynamic geomorphic readjustments of cobble-bedded streams as a result of flooding. Other studies show that HZs can dynamically change even without the channel-floodplain-scale geomorphic changes that accompany most major floods. *Marion et al.* [2002] demonstrated through flume experiments that different bed form shapes and sizes produce different rates of stream-subsurface exchange, thus resulting in different HZ geometry. Since bed forms are in dynamic equilibrium with flow conditions [*Allen*, 1982; *Southard and Boguchwal*, 1990], HZs can then be expected to evolve along with the bed forms as they respond to dynamic surface flow regimes. Our simulations suggest the possible dynamics between HZ geometry, streambed heterogeneity, and varying surface water conditions.

[26] Periodic pressure distributions in the streambed are set-up by topographic irregularities such as dunes and other typical bed forms. These pressure distributions are not exactly sinusoidal although it is not uncommon to idealize them as such. Examples of pressure distributions over triangular shaped obstructions, i.e., ripples and dunes, are given by *Vittal et al.* [1977] and *Shen et al.* [1990]. The wavelengths and heights of dunes are determined by flow parameters such as depth and velocity [*Yalin*, 1977; *Allen*, 1982]. Thus the sinusoidal head distributions that we consider can be thought of as a proxy for varying stream discharges. Although we did not monitor nor model flooding explicitly, we show indirectly a connection of flood and hyporheic zone dynamics through specifying various head boundaries representative of different bed form heights and lengths. Simulations that include a simple planar head boundary (pure longitudinal gradient with or without a

Figure 5. Simulation results showing increasing influence of heterogeneity from Figure 5a to Figure 5e. Dimensionless N (see explanation in text) and letter designations in Table 1 are shown beside the images.

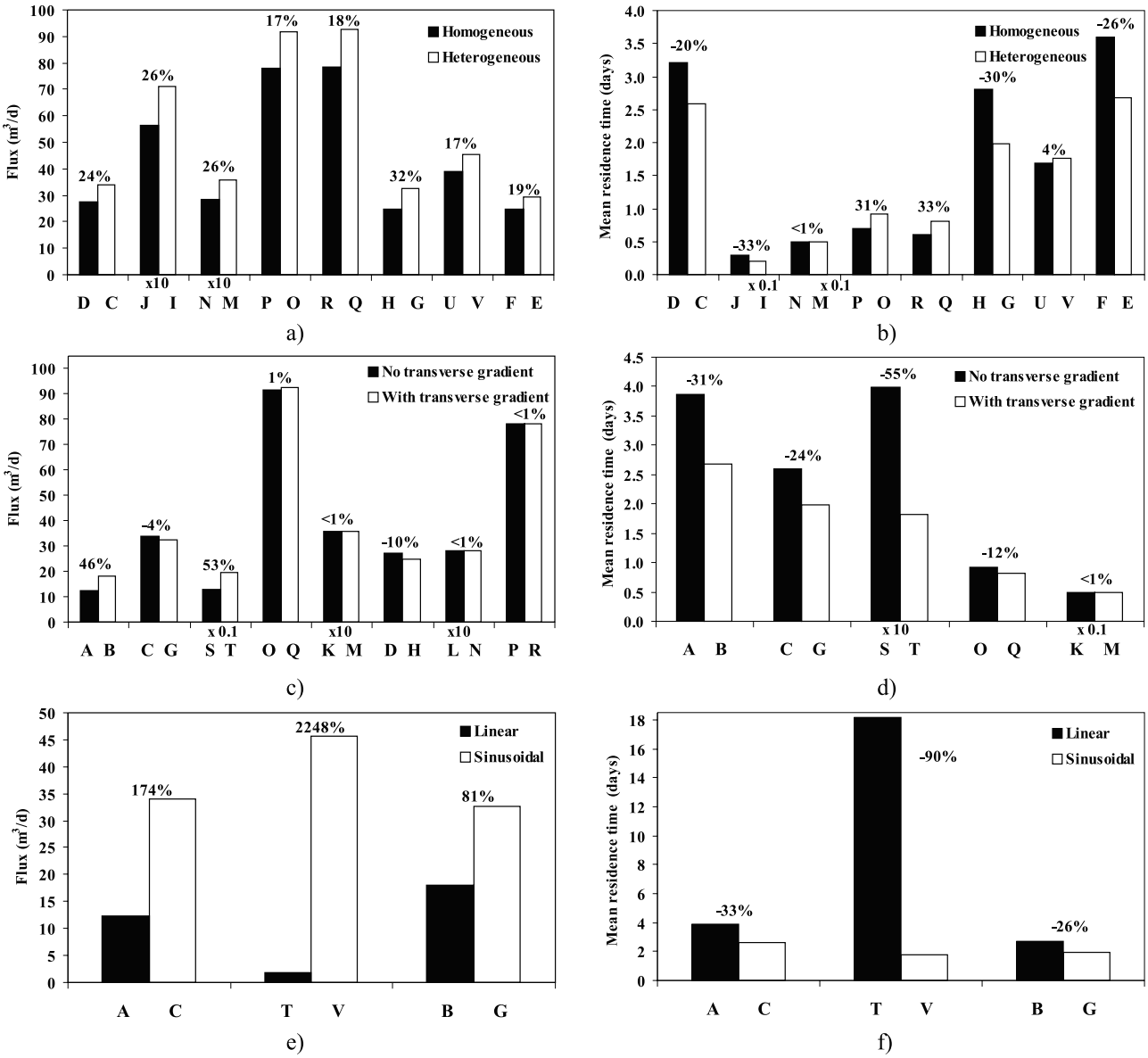

Figure 6. Comparison of steady state fluxes and mean residence times: (a and b) Homogeneous versus heterogeneous cases with similar (sinusoidal) head boundaries; (c and d) no transverse gradient versus with transverse gradient top boundary condition under similar K setting; (e and f) linear versus sinusoidal head top boundary condition under similar K setting. Here "$\times X$" in the x axis means that values were scaled X times to fit in the graph. Positive percentages in the graphs correspond to increases. Conditions for simulations as well as flux and residence time values are in Tables 1 and 2.

transverse gradient) are representative of conditions that favor the formation of lower stage and upper stage plane beds. Models that consider a sinusoidal head distribution are a proxy for flow conditions that generate dunes and antidunes. Unfortunately, our grid resolution prevented us from including fluctuations with centimeter-scale wavelengths, i.e., ripples. Nonetheless, we have shown that different surface flow conditions, represented by the different top boundaries, result in distinct HZ shapes. Such flow conditions may be present in different stages of a single flood. For example, a sequence of bed form states with increasing flow velocity is lower stage plane beds to dunes to upper stage plane beds or antidunes [*Bridge*, 2003]. Therefore the influence of heterogeneity on HZ configuration (and the value of dimensionless N) may vary through extremely short cycles.

3.3. Flux Calculations

[27] Steady state fluxes through the top boundary are given in Table 1 and illustrated in Figure 6 (since total flux "in" is approximately equal to total flux "out" through this boundary, the term "flux" herein refers only to influx). Comparison of cases with similar boundary conditions but different K fields (heterogeneous versus an equivalent homogenous medium, Figure 6a) shows that heterogeneity increases flux across the streambed. Flux enhancement ranges from 17%, for simulation V and its homogeneous equivalent (simulation U), to 32%, for simulations H and G.

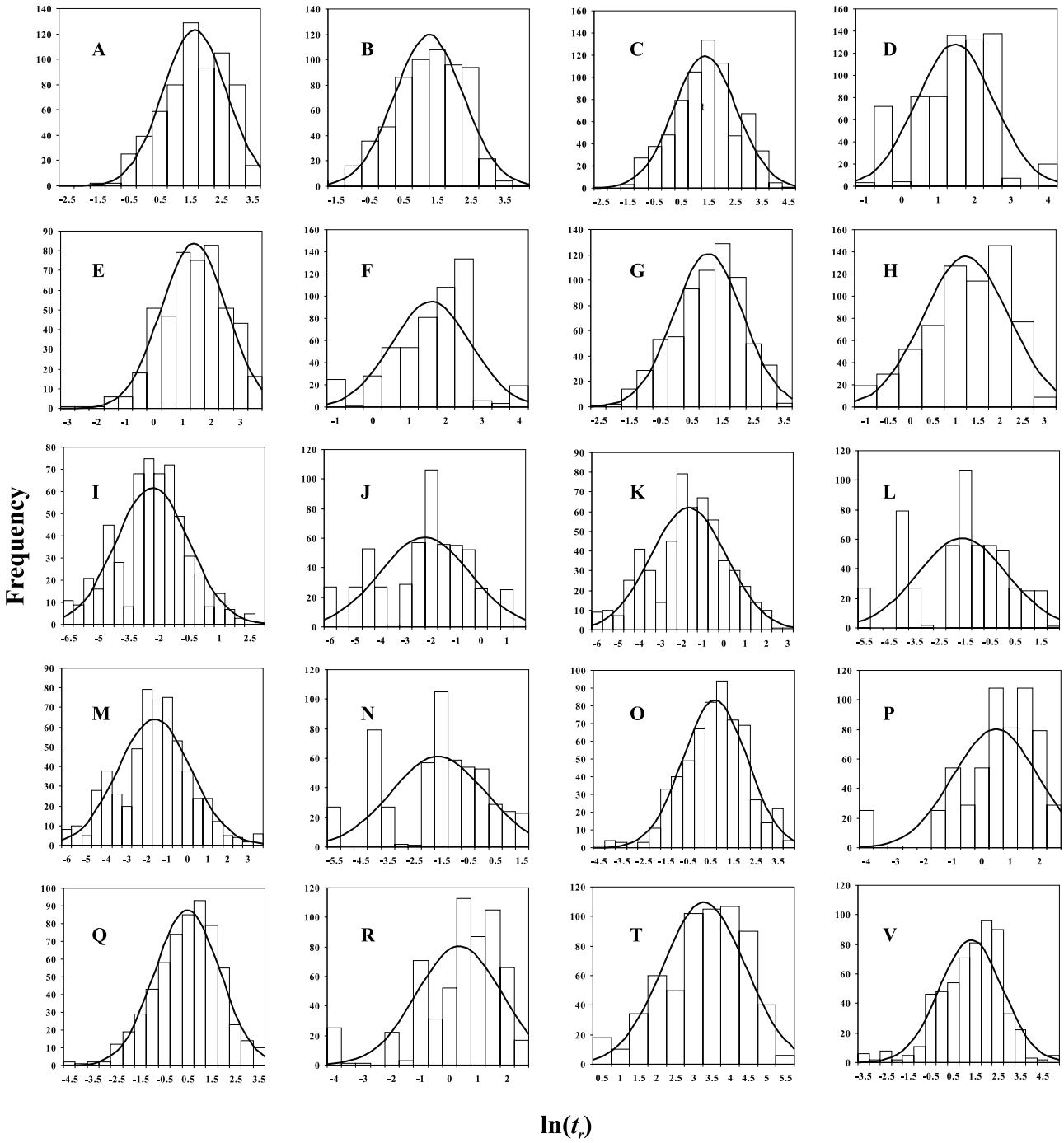

Figure 7. Histograms of natural logarithm of residence times plus fitted normal curves. Chart labels correspond to simulations in Tables 1 and 2.

As discussed previously, there is no flux under the conditions of a purely linear longitudinal gradient at the top boundary imposed on a homogenous K field. Consideration of heterogeneity under the same boundary conditions generates a flux of 12.4 m^3/d.

[28] The effects of an across-stream gradient depend on the presence of head fluctuations (Figure 6c). The flux changes only slightly for cases where the top constant head boundary is sinusoidal but it increases approximately 50% for cases where the top constant head boundary is linear (both A versus B and S versus T). The large increase in flux for the "linear" cases can be explained by the fact that the velocities are aligned along the direction of a high-K area in the domain [see *Cardenas and Zlotnik*, 2003a, Figures 1 and 7] when J_x is considered. The high-K area, whose deposition is determined by the superelevated surface water flow regime, acts as a preferential pathway. Since water surface topography and sediment distribution are strongly coupled along bends [*Bridge*, 1992], fluxes should be higher along similar portions of other river channels.

[29] Including a sinusoidal head boundary results in larger gradients and significant increases of flux (Figure 6e).

Table 2. Statistics of Residence Time Distributions (Natural Log Transformed and Standard Times)

Model[a]	Percent[b]	$\overline{\ln(t_r)}$	$\sigma_{\ln(t_r)}$	D	D_{crit}^{c}	$\overline{t_r}$, days	σ_{t_r}, days
A	58	1.87	1.02	0.054	0.065	3.87	8.84
B	65	1.51	1.03	0.052	0.066	2.67	6.20
C	68	1.64	1.17	0.033	0.062	2.59	8.87
D	77	1.72	1.05	0.089	0.063	3.22	7.89
E	84	1.63	1.14	0.037	0.075	2.67	8.34
F	100	1.85	1.07	0.103	0.072	3.59	9.40
G	53	1.30	1.11	0.059	0.063	1.98	5.70
H	53	1.49	0.95	0.096	0.064	2.81	5.35
I	100	−2.08	1.82	0.071	0.069	0.02	0.63
J	100	−2.01	1.78	0.132	0.07	0.03	0.64
K	100	−1.43	1.79	0.059	0.069	0.05	1.16
L	100	−1.36	1.77	0.115	0.07	0.05	1.21
M	93	−1.39	1.81	0.064	0.068	0.05	1.25
N	97	−1.37	1.76	0.118	0.07	0.05	1.17
O	96	0.94	1.43	0.036	0.067	0.92	6.64
P	100	0.73	1.48	0.139	0.067	0.70	5.81
Q	78	0.73	1.37	0.043	0.066	0.81	4.85
R	86	0.59	1.47	0.137	0.067	0.61	5.01
S	58	4.19	1.00	0.056	0.066	39.87	87.17
T	64	3.54	1.13	0.063	0.065	18.15	55.45
U	68	1.58	1.45	0.135	0.067	1.69	13.02
V	77	1.55	1.40	0.069	0.067	1.76	11.73

[a]Same as Table 1.
[b]Percent of total number of particles tracked that exit through the streambed, the rest exit through the sides.
[c]Critical value of Kolmogorov-Smirnov test statistic D for two-tailed test at $\alpha = 0.01$.

Superposition of even subtle sinusoidal head fluctuations on a small longitudinal gradient can result in a many fold increase in flux (T versus V in Table 1 and Figure 6e).

3.4. Mean Residence Times of Particles

[30] The HZ residence times, t_r, of water packets originating from the river were determined by computing total tracking times for 1215 regularly distributed particles originating from the top boundary. The residence time distributions are shown in Figure 7 and their statistics are summarized in Table 2. The distributions and statistics are biased. Particles with a total tracking time of zero (particles that are in upwelling or effluent areas) are excluded from the calculations. The residence times for the remaining particles are biased low. They are minimum values since some particles exit through the vertical faces of the domain and would move further in the HZ that is external to our modeled area (second column of Table 2). This is especially true in cases where we impose a transverse gradient (e.g., simulations B, G, and H shown in Figures 4b, 4e, and 4f), where as many as half of the particles exit through the sides of the domain.

[31] The residence time distributions are closely approximated by lognormal distributions (Figure 7). Lognormal curves describe the data better than exponential or normal curves, as is apparent in the Kolmogorov-Smirnov statistic D for the ln-transformed distributions (Table 2). One motivation of hyporheic exchange modeling is to replicate field observations of residence time distributions as well as the tailing in breakthrough curves of tracer pulses injected into the HZ. In previous studies, several probability density functions (PDFs) have been applied including lognormal, exponential, uniform, and Dirac delta distributions. These PDFs correspond to different site-specific scenarios and different exchange processes. However, it has been shown that exchange models based on advection are best represented by lognormal residence times PDFs [*Worman et al.*, 2002]. Our direct modeling of purely advective hyporheic exchange, as characterized by particle tracking, further illustrates this point. A lognormal PDF for residence times is typically attributed to a sinusoidal head distribution along the streambed [*Worman et al.*, 2002]. The residence time distribution of simulations A and B (Figure 7) are lognormally distributed, despite the absence of a sinusoidal head boundary (see Tables 1 and 2), showing that heterogeneity in K alone can result in lognormal residence time PDFs. However, it should be noted that only 58% and 65% of the particles used in determining residence times PDFs for simulations A and B exit through the top (see Table 2). It is difficult to discern how long (and what path) that the particles, that exit along domain sides, would have taken to return to the stream. These particles might remain in the subsurface until they encounter some heterogeneous inclusion, most likely a low-permeability zone, which will deflect them back toward the stream. Therefore our residence time distributions are biased toward shorter residence times corresponding to paths confined within the model domain. The actual distributions would presumably have longer tails.

[32] One would think that adding heterogeneity would increase residence time, t_r, especially under simple linear gradients, since the particles take a more tortuous path. However, Figure 6b shows that this is not always the case when the head distribution at the upper boundary is sinusoidal. Changes varied from a decrease of 33% to an increase of 33%. The lack of any noticeable trend in changes in t_r distributions owes to the complex interaction between the three-dimensionally variable head and hydraulic property distributions.

[33] The general effect of inclusion of a transverse gradient due to channel curvature is to decrease t_r (Figure 6d). Several particles exit the domain during early times through the left face (toward the point bar). Thus these times are biased and do not accurately represent residence times in the HZ since these particles, although outside the modeled domain, remain in the HZ. Decreases in t_r, which range from less than 1% to 55%, are observed in all comparative cases. These particles traverse longer paths in the longitudinal direction (Figures 4a and 4b illustrate this) when the transverse gradient is excluded.

[34] A sinusoidal top constant head boundary decreases t_r (Figure 6f). The river water packets/particles follow shorter routes (see Figures 3a and 3b) as a result of increased gradients per wavelength. As discussed in the previous section, these elevated gradients result in increased fluxes. The short residence times and large fluxes characteristic of this setting are ideal for circulating stream water more efficiently through the HZ. This has implications on the transport of ecologically important solutes and dissolved gases.

4. Summary

[35] We simulated hyporheic flow and transport through reconstructed heterogeneous streambed sediments and an equivalent homogeneous streambed. In addition to examining the impact of heterogeneity on hyporheic exchange,

we investigated the effects of boundary head sinusoidal fluctuations caused by surface water flow over bed forms and the effects of surface water topography resulting from channel curvature. The simulations show that the configuration of subchannel hyporheic zones is determined by both the pattern of heterogeneous streambed hydraulic conductivity and the space periodic head fluctuations at the top of the streambed. The relative importance of heterogeneity versus space periodic boundary head distributions are summarized by a dimensionless number that considers external forcing mechanisms (global and local head gradients) and internal control by heterogeneity. The results not only show that heterogeneity is more important when boundary head fluctuations are subdued but also has implications on the dynamic influence of heterogeneity on the hyporheic zone. The various head boundaries employed in our modeling efforts are proxies for different surface water conditions and bed form states that may occur during a single flood. We also found that an across-stream gradient, caused by flow along meander bends, deflects the hyporheic zone toward the cutbank. This deflection is magnified by the natural alignment of high-permeability areas in the streambed along the direction of maximum gradient.

[36] Flux calculations through the modeled streambed show that inclusion of heterogeneity can generate an increase in flux of 17 to 32% in the presence of bed forms represented by a space periodic head boundary. When the head distribution is approximately linear, such as when lower stage and upper stage plane beds are the dominant bed forms, flux into the hyporheic zone is entirely driven by heterogeneity. The effects of cross-stream gradients along meanders vary from miniscule additions in cases where the head boundary is space periodic to 46–53% increase in flux where the top boundary is planar. The larger increase under planar boundary head distributions is due to alignment of velocities with a geomorphologically controlled high-hydraulic conductivity lens. Superposition of a sinusoidally varying head boundary on a linear longitudinal gradient, over a heterogeneous streambed, increases flux by a factor of two to more than an order of magnitude.

[37] Residence times determined through forward tracking of particles originating from the stream bottom (top boundary) are closely approximated by a lognormal distribution. Mean residence times both increase and decrease when heterogeneity is considered and decrease when a space periodic head boundary is taken into consideration. Thus cycling of nutrient rich water is more effective in settings where sinusoidal head distributions are dominant because of the increased fluxes and decreased residence times. Mean residence times in subchannel HZs are smaller when the stream is flowing through a bend. Some of our residence time empirical distributions are biased by particles exiting through the sides of the domain, but remaining in the subsurface. A more accurate and systematic assessment of trends in residence time distributions will require a different approach.

[38] We explicitly show that heterogeneity, bed form configuration, and river bends have significant influence on subchannel hyporheic processes, in particular on hyporheic zone geometry, fluxes, and residence times. The relative importance of heterogeneity, bed form configuration and channel curvature is dynamic. The contribution of heterogeneity, relative to bed form configuration, can change from most to least dominant. This dominance is related to bed form amplitude and frequency which normally change through a single flood cycle. Hyporheic zone dynamics are better understood when heterogeneity, bed form configuration, and stream curvature are each included in models and field and laboratory observational programs.

[39] **Acknowledgments.** The initial stage of the project was funded by the USGS (grant 1434HQ96GR02683) and the Central Platte Natural Resources District, Nebraska. The first author was supported by the Frank E. Kottlowski Fellowship of the New Mexico Bureau of Geology and Mineral Resources at the New Mexico Inst. of Mining and Technology (NMIMT) during the duration of this study. Earlier versions of this manuscript benefited from comments by colleagues at NMIMT, namely Sam Earman and Enrique Vivoni and from insightful reviews by Judson Harvey, Steve Wondzell and Associate Editor Ellen Wohl.

References

Allen, J. R. L. (1982), *Sedimentary Structures, Their Character and Physical Basis*, volume I, *Dev. Sedimentol. Ser.*, vol. 30, Elsevier Sci., New York.

Bencala, K. E., and R. A. Walters (1983), Simulation of solute transport in a mountain pool-and-riffle stream: A transient storage model, *Water Resour. Res.*, *19*(3), 718–724.

Bridge, J. S. (1992), A revised model for water flow, sediment transport, bed topography and grain size sorting in natural river bends, *Water Resour. Res.*, *28*(4), 999–1013.

Bridge, J. S. (2003), *Rivers and Floodplains: Forms, Processes, and Sedimentary Record*, 491 pp., Blackwell, Malden, Mass.

Cardenas, M. B., and V. A. Zlotnik (2003a), Three-dimensional model of modern channel bend deposits, *Water Resour. Res.*, *39*(6), 1141, doi:10.1029/2002WR001383.

Cardenas, M. B., and V. A. Zlotnik (2003b), A simple constant-head injection test for streambed hydraulic conductivity estimation, *Ground Water*, *41*(6), 867–871.

Choi, J., J. W. Harvey, and M. H. Conklin (2000), Characterizing multiple scales of stream and storage zone interaction that affect solute fate and transport in streams, *Water Resour. Res.*, *36*(6), 1511–1518.

Doyle, M. W., E. H. Stanley, and J. M. Harbor (2003), Hydrogeomorphic controls on phosphorus retention in streams, *Water Resour. Res.*, *39*(6), 1147, doi:10.1029/2003WR002038.

Elliot, A. H., and N. H. Brooks (1997a), Transfer of nonsorbing solutes to a streambed with bed forms: Theory, *Water Resour. Res.*, *33*(1), 123–136.

Elliot, A. H., and N. H. Brooks (1997b), Transfer of nonsorbing solutes to a streambed with bed forms: Laboratory experiments, *Water Resour. Res.*, *33*(1), 137–151.

Findlay, S. (1995), Importance of surface-subsurface exchange in stream ecosystems: The hyporheic zone, *Limnol. Oceanogr.*, *40*(1), 159–164.

Harbaugh, A. W. (1990), A program for calculating subregional water budgets using results from the U.S. Geological Survey's modular three-dimensional finite-difference ground-water flow model, *U.S. Geol. Surv. Open File Rep., 90-392*, 27 pp.

Harvey, J. W., and K. E. Bencala (1993), The effect of streambed topography on surface-subsurface water exchange in mountain catchments, *Water Resour. Res.*, *29*(1), 89–98.

Harvey, J. W., and C. W. Fuller (1998), Effect of enhanced manganese oxidation in the hyporheic zone on basin-scale geochemical mass balance, *Water Resour. Res.*, *34*(4), 623–636.

Harvey, J. W., and B. J. Wagner (2000), Quantifying hydrologic interactions between streams and their subsurface hyporheic zones, in *Streams and Ground Waters*, edited by J. B. Jones and P. J. Mulholland, pp. 3–44, Academic, San Diego Calif.

Harvey, J. W., B. J. Wagner, and K. E. Bencala (1996), Evaluating the reliability of the stream tracer approach to characterize stream-subsurface water exchange, *Water Resour. Res.*, *32*(8), 2441–2451.

Ho, R. T., and L. W. Gelhar (1973), Turbulent flow with wavy permeable boundaries, *J. Fluid Mech.*, *58*(2), 403–414.

Jonsson, K., H. Johansson, and A. Worman (2003), Hyporheic exchange of reactive and conservative solutes in streams—Tracer methodology and model interpretation, *J. Hydrol.*, *278*(1–4), 153–171.

Kasahara, T., and S. M. Wondzell (2003), Geomorphic controls on hyporheic exchange flow in mountain streams, *Water Resour. Res.*, *39*(1), 1005, doi:10.1029/2002WR001386.

Larkin, R. G., and J. M. Sharp, Jr. (1992), On the relationship between river-basin geomorphology, aquifer hydraulics, and ground-water flow direction in alluvial aquifers, *Geol. Soc. Am. Bull.*, *104*, 1608–1620.

Marion, A., M. Bellinello, I. Guymer, and A. Packman (2002), Effect of bed form geometry on the penetration of nonreactive solutes into a streambed, *Water Resour. Res.*, *38*(10), 1209, doi:10.1029/2001WR000264.

Matos, J. E. R., C. Welty, and A. I. Packman (2003), Stream-groundwater interactions: The influence of aquifer heterogeneity and stream meandering on 2-D and 3-D hyporheic exchange flows, in *Proceedings of MODFLOW and More 2003: Understanding Through Modeling*, pp. 47–50, Int. Ground Water Model. Cent., Golden, Colo.

McDonald, M. G., and A. W. Harbaugh (1996), Programmer's documentation for MODFLOW-96, an update to the U.S. Geological Survey modular finite-difference ground-water flow model, *U.S. Geol. Surv. Open File Rep.*, *96-486*, 220 pp.

Packman, A. I., and K. E. Bencala (2000), Modeling surface-subsurface hydrological interactions, in *Streams and Ground Waters*, edited by J. B. Jones and P. J. Mulholland, pp. 45–80, Academic, San Diego Calif.

Packman, A. I., and N. H. Brooks (2001), Hyporheic exchange of solutes and colloids with moving bed forms, *Water Resour. Res.*, *37*(10), 2591–2605.

Pollock, D. W. (1994), User's guide for MODPATH/MODPATH-PLOT, version 3: A particle tracking post-processing package for MODFLOW, the U.S. Geological Survey finite-difference ground-water flow model, *U.S. Geol. Surv. Open File Rep.*, *94-464*, 234 pp.

Richardson, C. P., and A. D. Parr (1988), Modified Fickian model for solute uptake by runoff, *J. Environ. Eng.*, *114*(4), 792–809.

Runkel, R. L., D. M. McKnight, and H. Rajaram (2003), Modeling hyporheic zone processes, *Adv. Water Resour.*, *26*(9), 901–905.

Salehin, M., A. I. Packman, and M. Paradis (2003), Hyporheic exchange with heterogeneous streambeds: Laboratory experiments and modeling, *Eos Trans. AGU*, *84*(46), Fall Meet. Suppl., Abstract H42I-02.

Savant, S. A., D. D. Reible, and L. J. Thibodeaux (1987), Convective transport within stable river sediments, *Water Resour. Res.*, *23*(9), 1763–1768.

Shen, H. W., H. M. Fehlman, and C. Mendoza (1990), Bedform resistances in open channel flows, *J. Hydraul. Eng.*, *116*(6), 799–815.

Shum, K. T. (1992), Wave-induced advective transport below a rippled water-sediment interface, *J. Geophys. Res.*, *97*(C1), 798–808.

Sophocleous, M. (2002), Interactions between groundwater and surface water: The state of the science, *Hydrogeol. J.*, *10*(1), 52–67, doi:10.1007/s10040-001-0170-8.

Southard, J. B., and L. A. Boguchwal (1990), Bed configurations in steady unidirectional flows. Part 2. Synthesis of flume data, *J. Sediment. Petrol.*, *60*(5), 658–679.

Storey, R. G., K. W. F. Howard, and D. D. Williams (2003), Factors controlling riffle-scale hyporheic exchange and their seasonal changes in a gaining stream: A three-dimensional groundwater flow model, *Water Resour. Res.*, *39*(2), 1034, doi:10.1029/2002WR001367.

Thibodeaux, L. J., and J. D. Boyle (1987), Bed form-generated convective-transport in bottom sediments, *Nature*, *325*, 341–343.

Tóth, J. (1963), A theoretical analysis of groundwater flow in small drainage basins, *J. Geophys. Res.*, *68*(10), 4795–4812.

Triska, F. J., V. C. Kennedy, R. J. Avanzino, G. W. Zellweger, and K. E. Bencala (1989), Retention and transport of nutrients in third-order stream in northwestern California: Hyporheic processes, *Ecology*, *70*(6), 1893–1905.

Triska, F. J., J. H. Duff, and R. J. Avanzino (1993), The role of water exchange between a stream channel and its hyporheic zone in nitrogen cycling at the terrestrial-aquatic interface, *Hydrobiologia*, *251*(1–3), 167–184.

Vittal, N. K., K. G. Rangu Raju, and R. J. Garde (1977), Resistance of two-dimensional triangular roughness, *J. Hydraul. Res*, *15*(1), 19–36.

Wagner, F. H., and G. Bretschko (2002), Interstitial flow through preferential flow paths in the hyporheic zone of the Oberer Seebach, Austria, *Aquat. Sci.*, *64*(3), 307–316.

Waterloo Hydrogeologic, Inc. (2000), Visual MODFLOW v2.8.2 user's manual, 311 pp., Waterloo, Ontario, Canada.

White, D. S. (1993), Perspectives on defining and delineating hyporheic zones, *J. N. Am. Benthol. Soc*, *12*(1), 61–69.

Woessner, W. W. (2000), Stream and fluvial plain ground water interactions: Rescaling hydrogeologic thought, *Ground Water*, *38*(3), 423–429.

Wondzell, S. M., and F. J. Swanson (1996), Seasonal and storm dynamics of the hyporheic zone of a 4th-order mountain stream. 1. Hydrologic processes, *J. N. Am. Benthol. Soc.*, *15*(1), 3–19.

Wondzell, S. M., and F. J. Swanson (1999), Floods, channel change, and the hyporheic zone, *Water Resour. Res.*, *35*(2), 555–567.

Worman, A. (1998), Analytical solution and timescale for transport of reactive solutes in rivers and streams, *Water Resour. Res.*, *34*(10), 2703–2716.

Worman, A., A. I. Packman, H. Johansson, and K. Jonsson (2002), Effect of flow-induced exchange in hyporheic zones on longitudinal transport of solutes in streams and rivers, *Water Resour. Res.*, *38*(1), 1001, doi:10.1029/2001WR000769.

Wroblicky, G. J., M. E. Campana, H. M. Valett, and C. N. Dahm (1998), Seasonal variation in surface-subsurface water exchange and lateral hyporheic area of two stream-aquifer systems, *Water Resour. Res.*, *34*(3), 317–328.

Yalin, M. S. (1977), *Mechanics of Sediment Transport*, Pergamon, New York.

Young, P. C., and S. G. Wallis (1993), Solute transport and dispersion in channels, in *Channel Network Hydrology*, edited by K. Beven and M. J. Kirkby, pp. 129–174, John Wiley, Hoboken, N. J.

Zheng, C. (1999), MT3DMS, a modular three-dimensional multi-species transport model for simulation of advection, dispersion and chemical reactions of contaminants in groundwater systems; documentation and user's guide, *Contract Rep. SERDP-99-1*, 202 pp., U.S. Army Eng. Res. and Dev. Cent., Vicksburg, Miss.

M. B. Cardenas and J. L. Wilson, Department of Earth and Environmental Science, New Mexico Institute of Mining and Technology, Socorro, NM 87801, USA. (cardenas@nmt.edu)

V. A. Zlotnik, Department of Geosciences, University of Nebraska at Lincoln, Lincoln, NE 68588, USA.

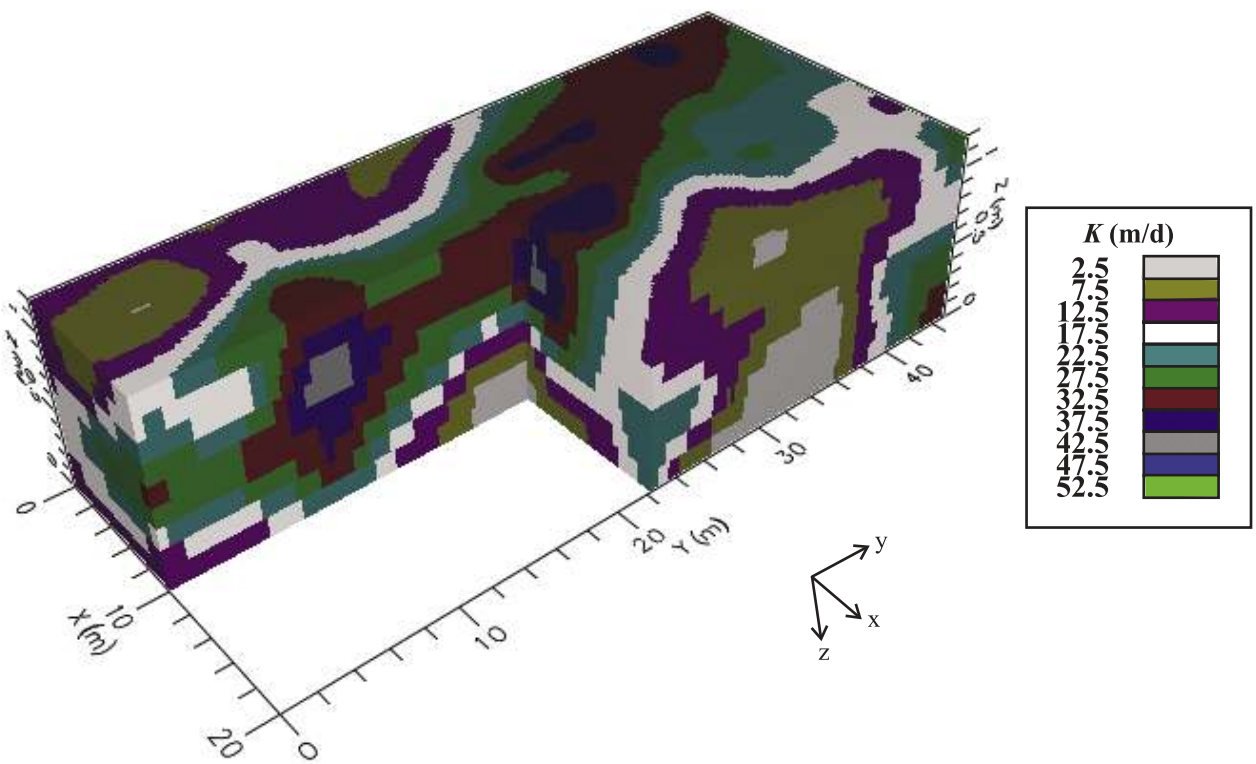

Figure 2. Model domain with three-dimensional hydraulic conductivity field.